**References and Notes**

1. G. Chuck, S. Hake, *Curr. Opin. Plant Biol.* **8**, 67 (2005).
2. C. Ferrándiz, Q. Gu, R. Martienssen, M. F. Yanofsky, *Development* **127**, 725 (2000).
3. M. A. Mandel, C. Gustafson-Brown, B. Savidge, M. F. Yanofsky, *Nature* **360**, 273 (1992).
4. D. Wagner, R. W. Sablowski, E. M. Meyerowitz, *Science* **285**, 582 (1999).
5. P. A. Wigge *et al.*, *Science* **309**, 1056 (2005).
6. M. Abe *et al.*, *Science* **309**, 1052 (2005).
7. J. W. Wang, B. Czech, D. Weigel, *Cell* **138**, 738 (2009).
8. A. Yamaguchi *et al.*, *Dev. Cell* **17**, 268 (2009).
9. C. Liu *et al.*, *Development* **134**, 1901 (2007).
10. S. J. Liljegren, C. Gustafson-Brown, A. Pinyopich, G. S. Ditta, M. F. Yanofsky, *Plant Cell* **11**, 1007 (1999).
11. V. Gregis, A. Sessa, C. Dorca-Fornell, M. M. Kater, *Plant J.* **60**, 626 (2009).
12. M. Ng, M. F. Yanofsky, *Plant Cell* **13**, 739 (2001).
13. F. Wellmer, M. Alves-Ferreira, A. Dubois, J. L. Riechmann, E. M. Meyerowitz, *PLoS Genet.* **2**, e117 (2006).
14. Materials and methods are available as supporting material on *Science* Online.
15. J. L. Riechmann, M. Wang, E. M. Meyerowitz, *Nucleic Acids Res.* **24**, 3134 (1996).
16. X. Y. Li *et al.*, *PLoS Biol.* **6**, e27 (2008).
17. J. L. Riechmann *et al.*, *Science* **290**, 2105 (2000).
18. M. J. Aukerman, H. Sakai, *Plant Cell* **15**, 2730 (2003).
19. M. Schmid *et al.*, *Development* **130**, 6001 (2003).
20. J. Mathieu *et al.*, *PLoS Biol.* **7**, e1000148 (2009).
21. C. Castillejo, S. Pelaz, *Curr. Biol.* **18**, 1338 (2008).
22. C. Liu, W. Xi, L. Shen, C. Tan, H. Yu, *Dev. Cell* **16**, 711 (2009).
23. V. Gregis, A. Sessa, L. Colombo, M. M. Kater, *Plant J.* **56**, 891 (2008).
24. K. Kaufmann *et al.*, *PLoS Biol.* **7**, e1000090 (2009).
25. V. V. Sridhar, A. Surendrarao, Z. Liu, *Development* **133**, 3159 (2006).
26. P. Achard *et al.*, *Curr. Biol.* **19**, 1188 (2009).
27. C. Gómez-Mena, R. Sablowski, *Plant Cell* **20**, 2059 (2008).
28. C. Gómez-Mena, S. de Folter, M. M. Costa, G. C. Angenent, R. Sablowski, *Development* **132**, 429 (2005).
29. W. J. Longabaugh, E. H. Davidson, H. Bolouri, *Dev. Biol.* **283**, 1 (2005).


30. We are grateful to T. Mastro for help with microarray hybridizations, S. Kushnir for generating AP1 antibodies, Y. Hanzawa and D. Bradley for providing transferred DNA (T-DNA) insertion lines, and E. Graciet for help with AP1-GR detection in nuclear extracts. This work was supported by grants from Science Foundation Ireland (06/IN.1/B851 to F.W.), European Union (EU)–Marie Curie program (Transistor-MRTNCT-2004–512285 to G.C.A. and IRG-224864 to J.L.R.), NSF (2010-0520193 to J.L.R. and E.M.M.), Spanish Ministerio de Ciencia e Innovación (BFU2008-04251 to J.L.R. and BIO2006-10994 and BIO2009-10876 to F.M.), and by the Millard and Muriel Jacobs Laboratory at Caltech. G.C.A. was also supported by the Netherlands Proteomics Centre and CBSG, which are part of the Netherlands Genomic Initiative. K.K. and J.M.M. were supported by fellowships from the EU–Marie Curie program; J.M.M. was also supported by CBSG and a Horizon grant (#93519020). T.F. was supported by a fellowship from CRAG. Microarray data have been deposited with the National Center for Biotechnology Information Gene Expression Omnibus under accession numbers GSE20184 and GSE20138 and the sequencing data under accession number GSE20176.


**Supporting Online Material**

www.sciencemag.org/cgi/content/full/328/5974/85/DC1
Materials and Methods
Figs. S1 to S11
Tables S1 to S12
References

26 November 2009; accepted 4 March 2010
10.1126/science.1185244

# Maize Tumors Caused by *Ustilago maydis* Require Organ-Specific Genes in Host and Pathogen

**David S. Skibbe,[1]* Gunther Doehlemann,[2]* John Fernandes,[1] Virginia Walbot[1]†**

**Infection of maize by corn smut (*Ustilago maydis*) provides an agronomically important model of biotrophic host-pathogen interactions. After penetration of the maize epidermis, fungal colonization of host tissue induces tumor formation on all aerial maize organs. We hypothesized that transformation of different primordia into plant tumors would require organ-specific gene expression by both host and pathogen and documented these differences by transcriptome profiling. Phenotypic screening of *U. maydis* mutants deleted for genes encoding secreted proteins and maize mutants with organ-specific defects confirmed organ-restricted tumorigenesis. This is the foundation for exploring how individual pathogen effectors, deployed in an organ-specific pattern, interact with host factors to reprogram normal ontogeny into a tumor pathway.**

*Ustilago maydis*, the causal agent of corn smut disease, is a basidiomycete fungus parasitizing only maize and its wild progenitor teosinte (both *Zea mays* L.) (*1*). *U. maydis* elicits large tumors on all aerial organs, where it completes pathogenic development by forming teliospores, its predominant dispersal agent (*1*). Unlike oncogenic agents that reactivate cell division, *U. maydis* is tumorigenic because fungal signals subvert normal programming of proliferating host cells, resulting in an extended period of plant cell division, chromosome endoreduplication, and cell expansion (*2*).

During the arms race with the multilayered plant defense system, plant pathogens such as *U. maydis* evolved a broad molecular repertoire to establish a compatible interaction (*3*). In contrast to necrotrophic pathogens that kill invaded cells and feed on debris, biotrophic pathogens establish an intimate interaction with living hosts (Fig. 1, A and B) by suppressing plant defenses while tapping the nutritional supply of colonized cells. This interaction is maintained by secretion of fungal effector proteins, which either act at the biotrophic interface between pathogen and plant cell or are translocated into the host cytoplasm (*3*). Sequencing of the *U. maydis* genome and transcriptome profiling during seedling infection identified 12 gene clusters encoding primarily uncharacterized, predicted secreted proteins expressed in planta (*4*). Infection assays with maize seedlings identified five of these clusters as functionally involved in tumor formation (*4*).

Extensive analysis of bacterial and oomycete effector proteins has identified several mechanisms for host cell manipulation (*5*); however, to date there is no evidence that the action or expression of any pathogen effector is tailored to individual host tissues. This is surprising because *U. maydis* is tumorigenic in leaves, stems, and flowers, and these organs and constituent maize tissues and cell types express distinctive developmental genes (*6*), as is true in any complex eukaryote. Furthermore, maize mutations that disrupt normal development can enhance or suppress tumor progression (*7*), demonstrating that host developmental status is important in the biotrophic interaction.

To define the genes expressed by maize and *U. maydis* during infections culminating in tumors (Fig. 1, C and D), transcriptomes were assessed on a microarray with probes to ~6700 annotated *U. maydis* genes (*4*), 4941 of which showed only background levels of hybridization with maize RNA in control hybridizations (i.e., high-confidence probes), and 36,800 maize genes, representing most gene models (*8*). Water-injected (mock infection) and fungal-infected organs were evaluated at 1 and 3 dpi (days postinjection) in seedling leaves and at 3 and 9 dpi in adult leaves and tassels (male reproductive inflorescences), as diagrammed in Fig. 1E (*9*).

Confirming previous reports (*10*, *11*), more than 30,000 maize genes were constitutively expressed (from mock 3-dpi samples), plus over 1500 organ-specific genes (table S1). Combined data from all three organs, comparing infected to mock samples, showed that 9207 (25%) unique maize transcripts were up-regulated (Fig. 2A) and 4455 (12%) were expressed only during fungal infection (Fig. 2B). At 3 dpi, *U. maydis* infection altered about one-third of the seedling leaf transcriptome: 4041 types were up-regulated or detected only in the infected sample ("on") (Fig. 2A), and 8111 transcript types were down-regulated or not detected in the infected sample ("off") (Fig. 2C). In adult leaves, more genes were up-regulated or on (6339) (Fig. 2A) than were down-regulated or off (3899) (Fig. 2C). In tassels,

[1]Department of Biology, Stanford University, Stanford, CA 94305–5020, USA. [2]Max Planck Institute for Terrestrial Microbiology, D-35043 Marburg, Germany.

*These authors contributed equally to this work.
†To whom correspondence should be addressed. E-mail: walbot@stanford.edu

only 7% of maize transcripts were altered by *U. maydis*, and the up or on (1118) (Fig. 2A) and down-regulated or off (1436) (Fig. 2C) classes were almost equivalent. Fungal infection alters only one-third as many genes in tassels, showing that formation of floral tumors was accompanied by less reprogramming of development compared to leaves (*12*).

Host responses were primarily organ-specific in both the up- and down-regulated classes. There were only 223 commonly up-regulated (Fig. 2A) and 23 on (Fig. 2B) transcripts. Although many genes were down-regulated or off among organs, only 135 were commonly down-regulated in all infected organs (Fig. 2C). We found differences in expression of defense-related genes in individual organs, e.g., the gene encoding pathogenesis-related protein 10 was strongly induced in seedling leaves but not in adult leaves. Hormone and metabolism genes were also differentially expressed during infection: gibberellic acid-oxidases, auxin transporter *pin1*, and auxin-response *tf-3* were up-regulated in adult but not in seedling leaves. These data establish that maize organs display discrete responses to *U. maydis* infection.

*U. maydis* expresses many genes during seedling infections, particularly the class encoding secreted proteins, which are not detected during saprophytic fungal growth (*4*). Notably, *U. maydis* exhibits expression patterns specific to infection location (Fig. 2D). Nearly one-third ($n$ =1353) of fungal transcripts were induced in all three organs, with another third ($n$ =1412) present in two organs. Almost 1200 fungal genes were uniquely expressed in adult leaves, with smaller numbers in seedling ($n$ = 296) and tassel ($n$ = 88). That more than 36% of the fungal transcriptome profile is organ-specific at 3 dpi suggests that successful host colonization requires deployment of gene products that can interact with maize proteins characteristic of three distinct developmental states. The specificity of interaction is also true at 9 dpi, when tumors are evident in adult leaves and tassels: In addition to 915 genes in common, *U. maydis* expresses 223 genes specifically in adult leaves and 714 in tassels (table S1).

There are 554 in silico–predicted secretory proteins encoded by *U. maydis*, collectively designated as the secretome (*13*); these are of particular interest for biotrophic fungal development. Most of these proteins were *U. maydis*–specific and lacked similarity to known enzymes (*13*). Of these, 325 were evaluated with high-confidence probes, resulting in the identification of 261 genes that were expressed in at least one infected versus mock sample type at 3 dpi (Fig. 2E). Only 21% ($n$ = 70) of these genes were expressed in all three maize organs at 3 dpi whereas 45% ($n$ = 118) showed organ-specific expression: 28 in seedling leaves, 86 in adult leaves, and 4 in tassels, a trend that continued at 9 dpi (Fig. 2F).

In a complementary approach, phenotypic screening of plant and fungal mutants tested the necessity of organ-specific host and *U. maydis* gene expression to make tumors. Maize mutants with defects in hormone signaling were scored for tumor formation in seedlings, adult leaves, and tassels as summarized in Table 1. *Dwarf8* (*D8*), which is disrupted in gibberellin hormone signaling, has drastically reduced shoot size (*14*). Infected *D8* seedlings support extensive tumor formation but completely lack adult tissue tumors (fig. S1A), indicating that gibberellin signaling is dispensable for tumor formation in seedlings but is indispensable in adult tissues. This observation is also consistent with the transcriptional induction of gibberellic acid-oxidases only in the adult tissue. Furthermore, the auxin hormone response mutant *sparse inflorescence1* (*spi1*) (*15*) shows normal vegetative tumors but essentially no floral tumors. The *Knotted1* (*Kn1*) mutant displays excessive adult leaf growth (*16*) from disrupted gibberellin regulation (*17*); *Kn1* has normal symptom formation in seedlings but displayed more frequent and larger adult leaf tumors and larger tassel tumors (Table 1 and fig. S1, B and C). Three premeiotic male-sterile mutants all produced normal seedling and adult leaf tumors but lacked floral organ tumors (Table 1). These observations demonstrate organ-specific control of tumor progression in maize growth control mutants.

To address the organ-specific role of *U. maydis* secretome proteins, deletion mutants in the SG200 solopathogenic strain for 12 gene clusters encod-

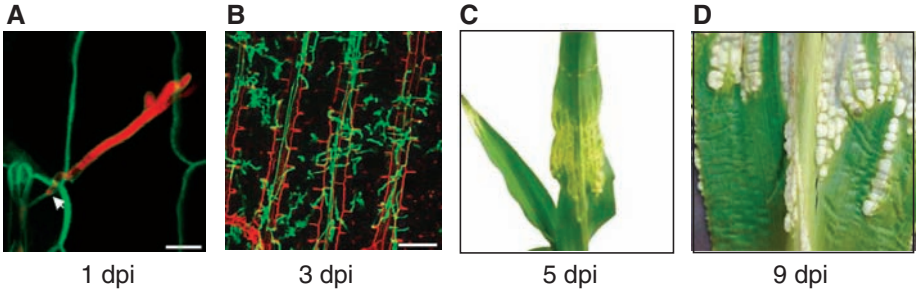


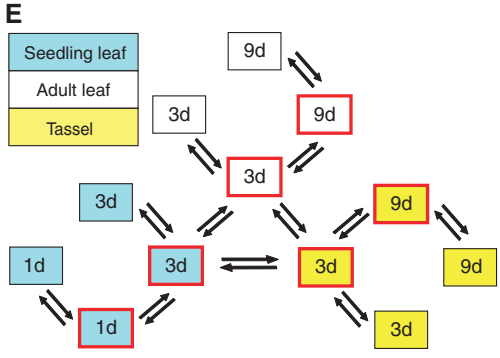


**Fig. 1.** Analysis of *U. maydis* infection and tumor progression. (**A**) Confocal microscopy at 1 dpi illustrates *U. maydis* hyphae (red) penetrating the seedling leaf epidermis that expresses the plasma-membrane marker PIN1A-YFP (yellow fluorescent protein) 15 (green) (*18*). Arrowhead indicates penetration site. Scale bar, 10 μm. (**B**) At 3 dpi, *U. maydis* hyphae (green, WGA-AF488 stained) proliferate inside seedling leaf tissue (red, plant cell wall autofluorescence). Scale bar, 50 μm. (**C** and **D**) Photographs illustrate the onset of tumor formation at 5 dpi (C) and evident tumors at 9 dpi (D). (**E**) Schema for the RNA profiling experiment. Each arrow represents a paired, two-color hybridization assay; the tail and arrowhead indicating cRNA samples labeled with Cy3 and Cy5 dyes, respectively. Samples were collected from plants injected with either *U. maydis* SG200 (outlined in red) or water at 1, 3, or 9 dpi.

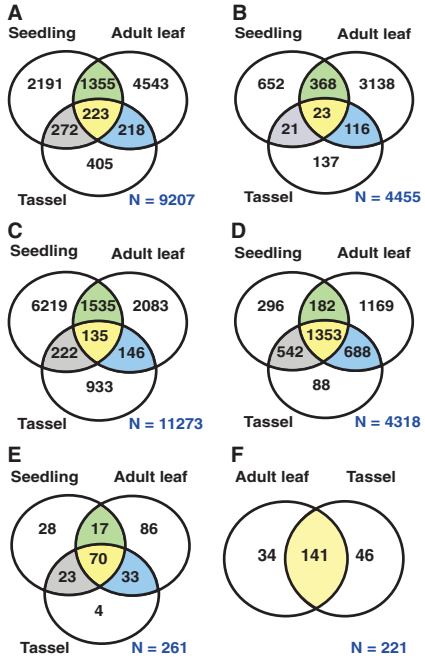


**Fig. 2.** Analysis of differentially expressed maize and *U. maydis* genes in infected versus mock-infected tissue at 3 dpi. The transcript sets of organ-specific (white), common to all organs (yellow), and shared between organs (green, seedling leaf and adult leaf; blue, adult leaf and tassel; gray, seedling leaf and tassel) are displayed in Venn diagrams. (**A**) Up-regulated plus now detected ("on") maize genes at 3 dpi. (**B**) Maize transcripts "on" at 3 dpi. (**C**) Down-regulated plus not detected ("off") maize genes at 3 dpi. (**D**) *U. maydis* transcripts expressed at 3 dpi. (**E**) *U. maydis* genes encoding secretome proteins at 3 dpi. (**F**) *U. maydis* genes encoding secretome proteins at 9 dpi. Tables S2 to S4 contain additional comparisons.

ing 71 secreted proteins (*4*) were inoculated on adult leaves and tassels of W23 inbred maize. In addition, all 12 mutants were reevaluated in W23 seedlings to confirm previous phenotypes reported on Golden Bantam corn (*4*). Five of the *U. maydis* mutants showed significantly different virulence depending on the organ infected: Δ5B was nonpathogenic (failed to penetrate beyond one cell) on seedlings (*3*) (Table 1); however, in adult leaves at 9 dpi, it caused extensive chlorosis spreading around infection sites indicative of successful fungal penetration (fig. S2C). Δ2A was hypervirulent on seedlings (*4*) but had a lower frequency and smaller tumors in adult leaves and a normal frequency of larger tumors in tassels (Table 1). Δ10A showed reduced frequency and size of seedling and adult leaf tumors but caused developmental arrest of the tassel, which formed no or only a few tiny tumors. The Δ9A mutant showed wild-type frequency of tumors on seedlings but exhibited reduced virulence on adult leaves and, similar to Δ10A, caused developmental arrest in tumor-free tassels (Table 1 and fig. S2, D and E). Most noteworthy are the findings for the Δ19A mutant deleted for 24 secretome proteins. This mutant did not cause any seedling tumors (*4*) but induced formation of tumors at a frequency comparable to that of SG200 in adult leaves and tassel, although the tumors were smaller (Table 1 and fig. S2F).

Consistent with these observations, the genes within the secretome clusters showed quantitative expression differences at 3 dpi in each maize organ (Fig. 3 and table S5). We found 39 organ-specific gene expression differences among the 47 secretome proteins contained in the five clusters with organ-specific phenotypes (Fig. 3). In particular, 15 genes of cluster 19A, which is essential for tumor formation in seedlings but dispensable in adult tissue, showed significantly reduced expression in tassel and adult leaves compared with seedling infections at 3 dpi, whereas only two genes showed increased expression in the tassel relative to seedlings (Fig. 3). In contrast, two genes of cluster 9A, which is more important for symptoms in adult tissue than in seedlings, were expressed at similar levels in all three organs.

Collectively, the gene expression and genetic findings demonstrate organ-specific expression of *U. maydis* effectors, showing essential roles in tumorigenesis. These secretome proteins, which likely constitute the majority of effector molecules eliciting host responses, indicate deployment of different "weapons" tuned to host organ properties. Smut fungi typically infect host seedlings and spread systemically in zones of proliferating cells during plant development; however, they cause symptoms exclusively in inflorescences (*18*). *U. maydis* is unique among smuts in converting leaves and stems into tumors; a larger suite of *U. maydis* genes is involved in tumor formation in vegetative organs than in the tassel. Floral tumors may draw on pathogenic factors that are more highly conserved with other fungi and that could serve general roles during pathogenesis in maize such as the *U. maydis* genes required for fungal penetration of plant cells (*19*).

Individual maize organs express distinctive proteins, and mutations that alter organ development can enhance or repress tumorigenesis by *U. maydis* (*7*) (Table 1). Mirroring the role of host differential gene expression is the unexpected transcriptional plasticity of *U. maydis* during infection of seedlings, adult leaves, and tassels and the observation that some deletion mutants alter tumor formation only in specific organs. We conclude that reprogramming by *U. maydis* may involve dedifferentiation from normal maize cell fates into new pathways, utilizing repression and de novo activation of different developmental programs in each infected proliferative zone.

We propose a model with two phases in this pathogenic interaction. First is establishment of compatibility, which most likely depends on universal pathogenicity factors to suppress plant defenses during fungal penetration (*12*, *20*).

**Table 1.** Organ-specific susceptibility to *U. maydis* in mutants. The solopathogenic SG200 strain was injected into W23 inbred or mutant maize lines in two greenhouse trials ($n$ = 16 or more mutant plants per trial) or in field trials ($n$ = 20 male sterile mutants) infected with FB1+FB2 (*7*). Responses in W23 and segregating (1:1) wild-type siblings were used as standards for judging the effect of maize mutants shown in the upper half of the table. Two trials were conducted in the greenhouse and three in the field for the fungal deletion strains in comparison to SG200 in infections of the W23 inbred as shown in the lower half of the table. Symptoms were highly consistent in trials summing to a minimum of $n$ = 40 per strain. *U. maydis* symptoms of infection, tumor frequency, and tumor size were scored 10 to 14 dpi (*8*) by two individuals; the mode is reported using a scale of 0 (no tumors), 1 (much fewer or far smaller tumors), 2 (smaller or fewer tumors), 3 (wild type), or 4 (higher frequency or larger than that of the wild type). Scoring integers different from "3" indicates significant differences in symptom formation compared to control experiments. Leaf number and tassel floral area affected (±SD) are reported.

| Genetic stock | Adult leaves [ave. no. with tumors (T) or symptoms (S)] | Adult leaf tumors: frequency, size | Tassel tumors (ave. % floral area area affected) | Tassel tumors: frequency, size |
|---|---|---|---|---|
| *Maize* | | | | |
| W23 control | T 4.0 ± 0.4 | 3, 3 | 55 ± 5 | 3, 3 |
| *Dwarf8* | 0* | 0, 0 | 0* | 0, 0 |
| *spi1* | T 4.6 ± 0.8 | 3, 3 | 4 ± 2* | 1, 1 |
| *Kn1* | T 4.9 ± 0.8 | 4, 4 | 65 ± 11 | 3, 4 |
| *mac1* | T 4.0 ± 1.0 | 3, 3 | 0* | 1, 1 on tassel stem |
| *msca1* | T 4.0 ± 0.8 | 3, 3 | 0* | 1, 1 on tassel stem |
| *ms23* | T 4.0 ± 0.8 | 3, 3 | 0* | 1, 1 on tassel stem |
| *U. maydis* | | | | |
| SG200 control | T 4.7 ± 1.0 | 3, 3 | 66 ± 12 | 3, 3 |
| Δ5B | S 2.0 ± 0.5* | 0, 0 | 0* | 0, 0 |
| Δ2A | T 4.6 ± 0.6 | 2, 2 | 69 ± 15 | 3, 4 |
| Δ10A | T 3.0 ± 0.4* | 1, 1 | 4 ± 2* | 1, 1 |
| Δ9A | T 4.5 ± 0.3 | 3, 2 | 44 ± 10 | 3, 2 |
| Δ19A | T 4.7 ± 0.6 | 3, 2 | 63 ± 13 | 3, 2 |

*$P$ < 0.05 compared with controls.

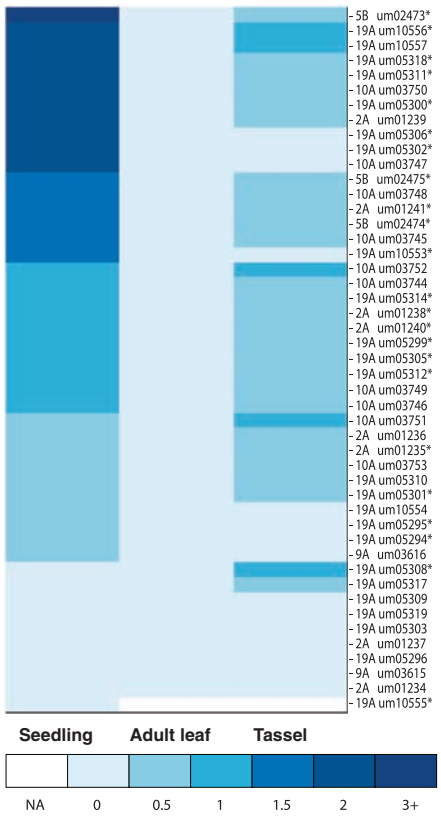


**Fig. 3.** Organ-specific expression of 47 *U. maydis* secretome genes contained within five gene clusters. The $\log_2$ ratio of normalized intensity divided by minimum normalized intensity for each probe is shown. The relative intensity of each gene among the tissues is displayed by shades of blue. White is used to represent genes without detectable expression. The chromosome and deletion cluster identifier (*4*) followed by the gene name are shown on the right. For the subset of 24 genes chosen for validation, statistically significant differences confirmed by quantitative reverse transcription–polymerase chain reaction are denoted by an asterisk.

Second, disease progression requires response to maize organ-specific properties so that *U. maydis* can tailor effector deployment to redirect physiology and development of a specific organ primordium. Sequential refinement of specificity may be of particular importance in this biotrophic interaction, which lasts 14 days from host penetration to fungal spore release. Within this conceptual framework, the next step is elucidation of distinct fungal and host factors interacting in a tissue-specific and temporal context. This new knowledge will clarify how organ-specific factors modulate biotrophy and, ultimately, tumor formation.


**References and Notes**

1. F. Banuett, in *Molecular Biology of Fungal Development*, H. D. Osiewacz, Ed. (Dekker, New York, 2002), pp. 349–398 (2002).
2. J. A. Callow, *New Phytol.* **75**, 253 (1975).
3. T. Boller, S. Y. He, *Science* **324**, 742 (2009).
4. J. Kämper *et al.*, *Nature* **444**, 97 (2006).
5. P. N. Dodds *et al.*, *New Phytol.* **183**, 993 (2009).
6. J. Ma, D. J. Morrow, J. Fernandes, V. Walbot, *Genome Biol.* **7**, R22 (2006).
7. V. Walbot, D. S. Skibbe, *Sex. Plant Reprod.* **23**, 1 (2010).
8. P. S. Schnable *et al.*, *Science* **326**, 1112 (2009).
9. Materials and methods and supporting materials are available on *Science* Online.
10. D. S. Skibbe, J. F. Fernandes, K. F. Medzihradszky, A. L. Burlingame, V. Walbot, *Plant J.* **59**, 622 (2009).
11. J. Fernandes, D. J. Morrow, P. Casati, V. Walbot, *Plant Biotechnol. J.* **6**, 782 (2008).
12. G. Doehlemann *et al.*, *Plant J.* **56**, 181 (2008).
13. O. Mueller *et al.*, *Fungal Genet. Biol.* **45** (suppl. 1), S63 (2008).
14. J. Peng *et al.*, *Nature* **400**, 256 (1999).
15. S. Barazesh, P. McSteen, *Trends Plant Sci.* **13**, 656 (2008).
16. L. G. Smith, B. Greene, B. Veit, S. Hake, *Development* **116**, 21 (1992).
17. N. Bolduc, S. Hake, *Plant Cell* **21**, 1647 (2009).
18. A. D. Martínez-Espinoza, M. D. García-Pedrajas, S. E. Gold, *Fungal Genet. Biol.* **35**, 1 (2002).
19. G. Doehlemann *et al.*, *PLoS Pathog.* **5**, e1000290 (2009).
20. F. L. W. Takken, W. I. L. Tameling, *Science* **324**, 744 (2009).



21. Research was supported by NSF grant IOS-0852788 (V.W.), the Savitzky Fund (D.S.S.), European Molecular Biology Organization STF program (G.D.), and Deutsche Forschungsgemeinschaft priority program FOR 666. We thank R. Kahmann for *U. maydis* strains. We appreciate critical comments on this manuscript by R. Kahmann, R. Fisher, and M. Barnett. Microarray data have been deposited in Gene Expression Omnibus (GEO) under accession GSE20130.


**Supporting Online Material**

www.sciencemag.org/cgi/content/full/328/5974/89/DC1
Materials and Methods
References
Figs. S1 and S2
Tables S1 to S6
References


9 December 2009; accepted 2 March 2010
10.1126/science.1185775


# Cryptic Sex-Ratio Bias Provides Indirect Genetic Benefits Despite Sexual Conflict


**Robert M. Cox* and Ryan Calsbeek**



When selection favors sexual dimorphism, high-fitness parents often produce low-fitness progeny of the opposite sex. This sexual conflict is thought to overwhelm the genetic benefits of mate choice because preferred males incur a cost through the production of low-fitness daughters. We provide a counterpoint in a lizard (*Anolis sagrei*) that exhibits sexual conflict over body size. By using mate-choice experiments, we show that female brown anoles produce more sons than daughters via large sires but more daughters than sons via small sires. Measures of progeny fitness in the wild suggest that maximal fitness payoffs can be achieved by shifting offspring production from daughters to sons as sire size increases. These results illustrate how the resolution of sexual conflict can restore the genetic benefits of mate choice.


Because of their divergent reproductive roles, males and females often experience different selection pressures acting on the same phenotypic traits (*1*). However, sharing a common genome constrains the sexes from evolving independently in response to these antagonistic selection pressures (*2*–*4*). This can result in a genomic tug of war referred to as intralocus sexual conflict (*5*–*7*). When such conflict is widespread throughout the genome, high-fitness parents may actually produce low-fitness progeny of the opposite sex (*8*–*14*). This outcome can override the potential genetic benefits of mate choice because preferred males incur a net fitness cost through the production of low-fitness daughters (*8*–*10*). When sire genotypes have differential fitness effects on sons versus daughters, females are predicted to alter progeny sex ratio accordingly (*15*). We tested whether progeny sex-ratio bias can facilitate the sex-specific inheritance of good genes, thereby preserving the genetic benefits of mate choice in the face of sexual conflict.

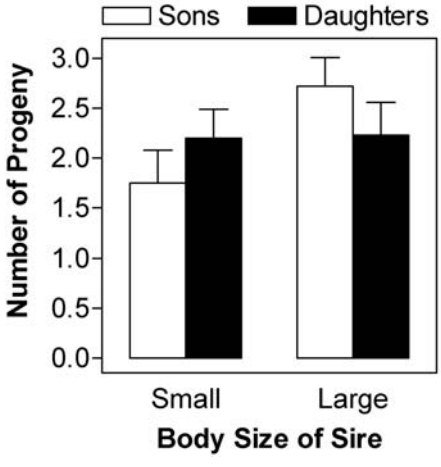


**Fig. 1.** Female anoles bias progeny sex ratio as a function of sire body size. Data are least-squares means ± 1 SEM from analyses weighted by the total number of progeny produced by each dam-sire pair. Size is dichotomized relative to the population mean.

The brown anole lizard (*Anolis sagrei*) exhibits signatures of intralocus sexual conflict over body size (fig. S1). On average, adult males are 30% longer and 150% heavier than adult females (*16*). Selection creates the potential for sexual conflict by favoring large size in males and intermediate size in females (*17*). However, anoles have also evolved several mechanisms that may resolve this conflict. First, body size and other morphological traits are heritable within each sex but exhibit negative genetic correlations between the sexes (*18*). Second, paternity analyses of wild populations reveal that females produce more sons via large sires but more daughters via small sires (*18*). This suggests a form of cryptic sex-ratio bias that may allow females to adaptively sort genes with sex-specific fitness effects into sons and daughters.

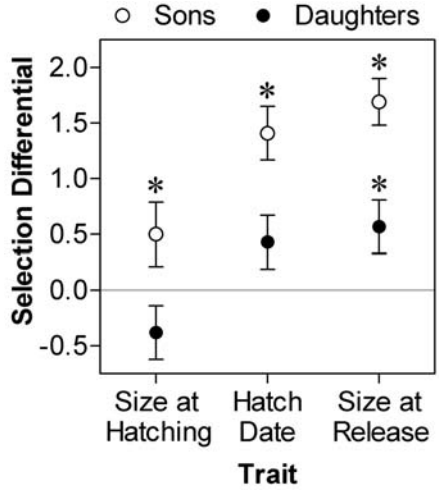


**Fig. 2.** Natural selection on three phenotypic traits differs between male and female progeny. Data are selection differentials ± 1 SEM derived from regressions of relative survival on trait values standardized to the population mean in unit variance. Asterisks indicate statistical significance ($P < 0.05$) on the basis of logistic regression.


Department of Biological Sciences, Dartmouth College, Hanover, NH 03755, USA.

*To whom correspondence should be addressed. E-mail: robert.m.cox@dartmouth.edu